MOLECULAR AND CELLULAR BIOLOGY, June 2006, p. 4511–4518 Vol. 26, No. 12
0270-7306/06/$08.00+0 doi:10.1128/MCB.00238-06

Essential Role of *Pten* in Body Size Determination and Pancreatic β-Cell Homeostasis In Vivo

Kinh-Tung T. Nguyen,[1] Panteha Tajmir,[1] Chia Hung Lin,[1] Nicole Liadis,[1] Xu-Dong Zhu,[1] Mohammed Eweida,[1] Gunce Tolasa-Karaman,[2] Fang Cai,[2] Rennian Wang,[3] Tadahiro Kitamura,[4] Denise D. Belsham,[2] Michael B. Wheeler,[2] Akira Suzuki,[5] Tak W. Mak,[1,6] and Minna Woo[1,7]*

Department of Medicine, Medical Biophysics, Institute of Medical Science, Ontario Cancer Institute, University of Toronto, Toronto, Ontario, Canada[1]; Department of Physiology, University of Toronto, Toronto, Ontario, Canada[2]; Department of Physiology and Pharmacology, University of Western Ontario, London, Ontario, Canada[3]; Department of Medicine, Columbia University, New York, New York[4]; Department of Molecular Biology, Akita University School of Medicine, Akita, Japan[5]; The Advanced Medical Discovery Institute and The Campbell Family Institute for Breast Cancer Research, Toronto, Ontario, Canada[6]; and Department of Medicine, St. Michael's Hospital, Toronto, Ontario, Canada[7]

Received 8 February 2006/Returned for modification 21 March 2006/Accepted 30 March 2006

PTEN (phosphatase with tensin homology) is a potent negative regulator of phosphoinositide 3-kinase (PI3K)/Akt signaling, an evolutionarily conserved pathway that signals downstream of growth factors, including insulin and insulin-like growth factor 1. In lower organisms, this pathway participates in fuel metabolism and body size regulation and insulin-like proteins are produced primarily by neuronal structures, whereas in mammals, the major source of insulin is the pancreatic β cells. Recently, rodent insulin transcription was also shown in the brain, particularly the hypothalamus. The specific regulatory elements of the PI3K pathway in these insulin-expressing tissues that contribute to growth and metabolism in higher organisms are unknown. Here, we report PTEN as a critical determinant of body size and glucose metabolism when targeting is driven by the rat insulin promoter in mice. The partial deletion of PTEN in the hypothalamus resulted in significant whole-body growth restriction and increased insulin sensitivity. Efficient PTEN deletion in β cells led to increased islet mass without compromise of β-cell function. Parallel enhancement in PI3K signaling was found in PTEN-deficient hypothalamus and β cells. Together, we have shown that PTEN in insulin-transcribing cells may play an integrative role in regulating growth and metabolism in vivo.

The phosphoinositide 3-kinase (PI3K) pathway is a key signaling cascade that is activated in response to growth factors such as insulin and insulin-like growth factor 1 (IGF-1) (30). PTEN (phosphatase with tensin homology) is a dual-specificity phosphatase that dephosphorylates phosphatidylinositol 3,4,5-trisphosphate to phosphatidylinositol-4,5-bisphosphate and thus is a potent antagonist of PI3K signaling (32, 35). Although initially discovered as a tumor suppressor with a regulatory role in cell survival and proliferation, particularly in tumor-prone tissues such as the breast and endometrium (33), more recent studies have highlighted a role for PTEN in metabolism (5). Tissue-targeted ablation in fat, muscle, and liver generally led to improved insulin sensitivity in these classical peripheral insulin target tissues (13, 19, 36, 41). Furthermore, *Pten* has been implicated in determining differentiated cellular function in other tissues, such as the cardiomyocytes and lymphocytes (7, 38). This wide array of distinct PTEN function is highly tissue and context dependent.

Tissue-specific genetic targeting strategies have shown signaling molecules of the insulin- and/or IGF-1-PI3K pathway to play a critical role in β-cell mass and function. β-Cell-specific deletion of the insulin or IGF-1 receptor leads to impaired differentiated β-cell function (16, 17), while insulin receptor substrate 2 (IRS-2) appears to be a key factor in β-cell mass determination (12, 15, 23, 42). Constitutive overexpression of protein kinase B/Akt leads to increased islet mass, β-cell proliferation, and protection from experimental diabetes (3, 40). Recent reports have shown that the insulin promoter commonly used to genetically target genes of interest in β cells also promotes gene expression in the brain in mammals, particularly within the hypothalamus (9, 10). The population of neurons that expresses the insulin promoter appears to be a novel subset of hypothalamic neurons and is currently not yet characterized (6). The biological significance of these insulin-producing neurons is also not well understood, and the roles of the regulatory elements of PI3K signaling within this unique insulin-transcribing neuron are not known.

In order to study the role of PTEN in these insulin-producing cells in the brain and β cells, we have used the rat insulin promoter to drive the deletion of PTEN using the Cre-loxP system. Using this genetic approach, we achieved efficient deletion of PTEN in β cells and partial deletion of PTEN in the hypothalamus. These mutations in mice had a profound effect on body size and β-cell mass, showing a potential integrative role of PTEN in growth and metabolism.

* Corresponding author. Mailing address: Princess Margaret Hospital, 8th Floor, Room 8-113, Toronto, Ontario, Canada M5G 2M9. Phone: (416) 946-4501, ext. 3971. Fax: (416) 946-2086. E-mail: mwoo@uhnres.utoronto.ca.

MATERIALS AND METHODS

Mice. *Pten*$^{fl/fl}$ mice, with exons 4 and 5 of *Pten* flanked by loxP sites by homologous recombination (32), were mated with mice carrying the Cre transgene under the control of the rat insulin 2 promoter [TgN(ins2-*cre*)25Mgn,

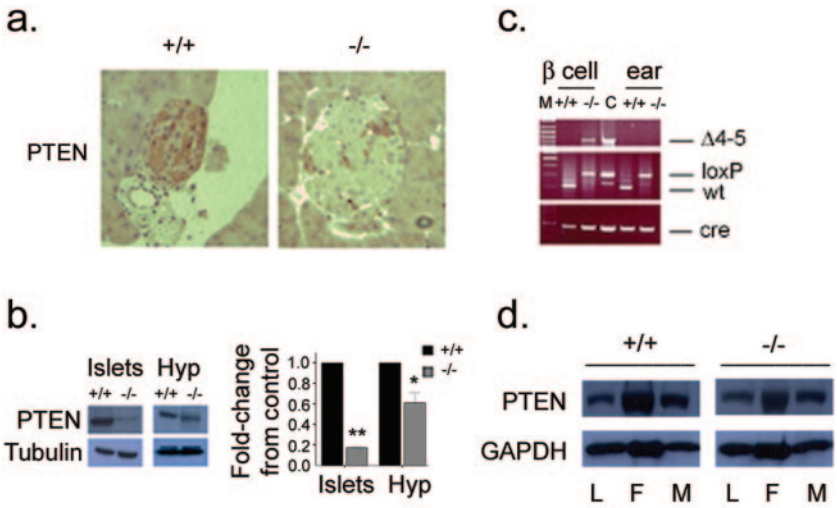

FIG. 1. Tissue-specific deletion of *Pten*. (a) Immunohistochemistry showing PTEN deletion in β cells (original magnification, ×25). (b) Western blots (left panels) and quantification of Western blot signal (right panel) showing decreased expression of PTEN in isolated islets and the hypothalamus (Hyp). Residual signal in islets is likely due to the presence of non-β cells. *, $P = 0.011$; **, $P < 0.005$. The error bar indicates the standard error of the mean. (c) PCR analysis of Cre-mediated recombination of the *Pten* locus (Δ4-5, top) in β cells and ear tissue and genotyping for *Pten*-loxP allele (middle) and Cre (bottom). M, marker; C, control mammary gland tumor; wt, wild type. (d) Expression of PTEN in liver (L), fat (F), and muscle (M) is unchanged. +/+, RIP*cre*$^{+}$ *Pten*$^{+/+}$ mice; −/−, RIP*cre*$^{+}$ *Pten*$^{fl/fl}$ mice.

hereafter referred to as RIP*cre*; Jackson Laboratories]. RIP*cre*$^{+}$ *Pten*$^{+/fl}$ mice were intercrossed to generate RIP*cre*$^{+}$, RIP*cre*$^{-}$ *Pten*$^{fl/fl}$, *Pten*$^{+/+}$, and *Pten*$^{+/fl}$ mice. Genotyping was performed with PCR using ear clip DNA as previously described (41). Mice were maintained on a mixed 129J-C57BL/6 background, and only littermates were used as controls as indicated. All mice were housed in a pathogen-free facility on a 12-h light-dark cycle and were fed ad libitum with standard irradiated rodent chow (5% fat; Harlan Teklad, Indianapolis, IN) in accordance with the Ontario Cancer Institute Animal Care Facility protocol. All litters were weaned at 4 weeks of age. The activity of the animals was not restricted.

Metabolic studies and hormone measurements. All overnight fasts were 14 to 16 h in duration. All blood glucose levels were determined from tail venous blood with an automated glucose monitor (One Touch II; Lifescan, Inc., Milpitas, CA). Food intake was measured by housing animals singly, with determinations of the differences in food weight at the beginning and end of a 7-day period. Relative daily food intake was subsequently calculated by dividing daily food weight by mouse weight at the start of the 7-day period. Glucose tolerance tests were performed on overnight-fasted animals between 8 and 10 a.m., utilizing a glucose dose of 1 g/kg of body weight injected intraperitoneally (i.p.) and measurements of glucose levels at 0, 15, 30, 60, and 120 min after the injection. Insulin tolerance tests were performed on random-fed animals between 8 and 10 a.m., utilizing human regular insulin (Novo Nordisk) at a dose of 0.5 U/kg body weight, and blood glucose levels were measured at 0, 15, 30, 45, and 60 min after the injection. Glucose-stimulated insulin secretion was performed on overnight-fasted animals after an injection of glucose i.p. at a dose of 3 g/kg body weight, with tail vein blood collected at 0, 2, and 30 min after the injection. Insulin levels were measured by an enzyme-linked immunosorbent assay kit using a rat insulin standard (Crystal Chem, Downers Grove, IL). Growth hormone (GH), IGF-1, and corticosterone levels were measured by the Mouse Metabolic Phenotyping Center, Hormone Analytical Subcore Unit (Vanderbilt University, Nashville, TN). Pancreatic insulin content was determined by acid ethanol extraction using an insulin radioimmunoassay kit (Linco). Pancreatic perfusion was performed as previously described (14), with the following modifications: random-fed mice were anesthetized with Avertin, and perfusion of the pancreas followed five phases. The preparatory phase with the perfusate 2.8 mM glucose lasted 15 min, followed by 2.8 mM glucose for 5 min, 16.7 mM glucose for 15 min, 2.8 mM glucose for 5 min, and ending with arginine plus 16.7 mM glucose stimulation for 6 min. Effluents were collected every minute, and samples were stored at −20°C until analysis for insulin concentration by radioimmunoassay. Insulin levels were normalized for collected volume at each time point.

Islet isolation and β-cell sorting. Pancreatic islets were isolated from 4-to-8-week-old mice as previously described (21). Briefly, 3 ml collagenase (3 mg/ml; Sigma, St. Louis, MO) was injected into the pancreatic duct and pancreatic tissue was gently removed and digested in collagenase solution at 37°C with shaking for 10 to 15 min. The digestion was stopped by ice-cold Hanks' balanced salt solution containing 10% fetal calf serum, and the tissue was washed several times with ice-cold Hanks' balanced salt solution and passed through a filter. Islets were then handpicked under a dissecting microscope. For β-cell sorting, freshly isolated islets were dispersed and subjected to flow cytometry to purify β cells on the basis of high autofluorescence as previously described by Darwiche et al. (8).

Western blotting and RT-PCR. Islets or the hypothalamus was isolated and protein lysates were obtained as previously described (41). The lysates were separated by sodium dodecyl sulfate-10% polyacrylamide gel electrophoresis and then immunoblotted with antibodies to PTEN (NeoMarker, Fremont, CA), AKT, phospho-AKT (Ser473), phospho-FoxO-1, and phospho-GSK3β (Cell Signaling Technology, Beverly, MA), IRS-2, phospho-IRS-2, and total FoxO-1 (Santa Cruz Biotechnology, Santa Cruz, CA), GLUT2 (Chemicon, Temecula, CA), and PDX-1 (gift of Chris Wright). Western blot signal densities were analyzed using NIH Image software. mRNA was extracted from the hypothalamus by TRIzol reagent by following the manufacturer's protocol (Invitrogen, Toronto, Ontario, Canada). Semiquantitative reverse transcription-RT (RT-PCR) amplification was performed with a one-step RT-PCR kit (QIAGEN, Toronto, Ontario, Canada; primer sequences available upon request). Densitometric analysis was performed using a Kodak imaging system (Kodak IS2000R; Eastman Kodak Company, Rochester, NY). Transcript levels were normalized for β-actin and expressed in arbitrary units relative to littermate control levels.

Immunohistochemistry, immunofluorescent staining, and islet morphometry. Pancreatic tissue was fixed for 24 h in 4% paraformaldehyde in 0.1 M phosphate-buffered saline (pH 7.4). Samples were dehydrated and prepared as paraffin blocks. Seven-micrometer-thick sections were obtained at 100-to-150-μm intervals on at least three levels and stained with hematoxylin and eosin and insulin (DAKO), glucagon (NovoCastra Laboratories), synaptophysin (Boehringer Mannheim), laminin (Sigma), β-catenin (BD Transduction Laboratories), and Ki67 (DAKO). Additionally, immunohistochemistry was performed to detect AKT, phospho-AKT, and GLUT2 (antibodies noted under "Western blotting and RT-PCR" above). Immunofluorescence staining was performed using insulin (DAKO), PDX-1 (gift of C. Wright), and FoxO-1 (gift of D. Accili) and counterstained with 4′-6-diamidino-2-phenylindole (DAPI) (Sigma). Total islet area and total pancreatic area were determined on synaptophysin-stained sections as previously described (21) and expressed as total islet area divided by total pancreatic area. β-Cell size was determined by examining sections stained by immunofluorescence for insulin and DAPI using a Zeiss inverted microscope, with photographs of 6 to 12 representative islets per sample at ×40 magnification. The insulin-stained area was then determined using Image-Pro Plus software (Media Cybernetics, Silver Spring, MD) and divided by the number of DAPI-positive nuclei within the insulin-stained areas.

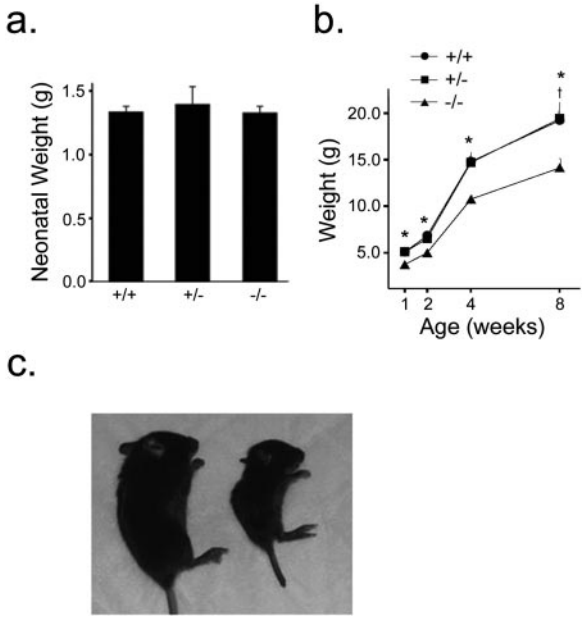

FIG. 2. RIP*cre*$^{+}$ *Pten*$^{fl/fl}$ mice show growth restriction from the early postnatal period onward. (a) Neonatal birth weights of RIP*cre*$^{+}$ *Pten*$^{fl/fl}$ mice are similar to birth weights of littermate controls on postnatal day 1 ($n \geq 3$ per genotype). (b) Growth of RIP*cre*$^{+}$ *Pten*$^{fl/fl}$ mice is restricted compared with that of RIP*cre*$^{+}$ *Pten*$^{+/+}$ and RIP*cre*$^{+}$ *Pten*$^{+/-}$ littermates from 1 week of age onward ($n \geq 14$). *, $P \leq 0.005$ for comparison between RIP*cre*$^{+}$ *Pten*$^{fl/fl}$ and RIP*cre*$^{+}$ *Pten*$^{+/+}$ or RIP*cre*$^{+}$ *Pten*$^{+/-}$; †, $P = 0.01$ for RIP*cre*$^{+}$ *Pten*$^{fl/fl}$ versus RIP*cre*$^{+}$ *Pten*$^{+/-}$ mice. (c) Growth-restricted RIP*cre*$^{+}$ *Pten*$^{fl/fl}$ mice (right) are proportionately smaller than littermate RIP*cre*$^{+}$ *Pten*$^{+/+}$ mice (left, 4 weeks old). Error bars indicate standard errors of the means. +/+, RIP*cre*$^{+}$ *Pten*$^{+/+}$ mice; −/−, RIP*cre*$^{+}$ *Pten*$^{fl/fl}$ mice; +/−, RIP*cre*$^{+}$ *Pten*$^{+/fl}$ mice.

Streptozotocin protocol. Multiple low doses of streptozotocin (MLDS) were injected into mice as previously described (21). Blood glucose was measured weekly after MLDS injection, and RIP*cre*$^{+}$ *Pten*$^{fl/fl}$ and control mouse pairs were sacrificed for pancreatic examination by hematoxylin and eosin and terminal deoxyribonucleotide transferase-mediated dUTP nick end labeling (TUNEL) staining as soon as one or both mice of the pair developed blood glucose levels greater than 20.0 mmol/liter.

Statistical analysis. Data are presented as means ± standard errors of the mean and were analyzed by the one-sample *t* test, independent-samples *t* test, and one-way analysis of variance with the post-hoc Tukey least significant difference test where appropriate. All data were analyzed using the statistical software package SPSS (version 11.0) for Macintosh.

RESULTS

Generation of RIPcre^{+} *Pten*$^{fl/fl}$ mice. Mice lacking PTEN in the hypothalamus and β cells were generated by breeding animals harboring exons 4 and 5 of the *Pten* gene flanked by loxP sites (*Pten*$^{fl/fl}$) (32) to mice expressing the Cre transgene under the rat insulin promoter (29) (hereafter referred to as RIP*cre*$^{+}$). In keeping with previous reports (9), we observed a partial deletion of PTEN in the hypothalamus and the efficient deletion of PTEN in β cells (Fig. 1a and b). PCR analysis of purified β cells confirmed the presence of the deleted allele in RIP*cre*$^{+}$ *Pten*$^{fl/fl}$ β cells (Fig. 1c). The expression of PTEN in liver, fat, and muscle was unaffected (Fig. 1d).

RIPcre^{+} *Pten*$^{fl/fl}$ mice demonstrate postnatal growth restriction independently of food intake and the GH/IGF-1 axis. RIP*cre*$^{+}$ *Pten*$^{fl/fl}$ mice were born at Mendelian frequencies, and neonatal birth weights were similar between RIP*cre*$^{+}$ *Pten*$^{fl/fl}$ mice and RIP*cre*$^{+}$ *Pten*$^{+/+}$ or RIP*cre*$^{+}$ *Pten*$^{+/fl}$ littermate controls (Fig. 2a). However, starting at about 1 week of age, the growth of almost all of the RIP*cre*$^{+}$ *Pten*$^{fl/fl}$ mice was significantly impaired compared with that of the RIP*cre*$^{+}$ *Pten*$^{+/+}$ and RIP*cre*$^{+}$ *Pten*$^{+/fl}$ mice (Fig. 2b). The growth restriction was proportionate, as weight-matched nonlittermate controls had similar snout-to-anus lengths and solid organ weights (Fig. 2c and data not shown). A significant proportion of the small RIP*cre*$^{+}$ *Pten*$^{fl/fl}$ mice (57%; 124 of 214 RIP*cre*$^{+}$ *Pten*$^{fl/fl}$ pups born) died prematurely, prior to 5 weeks of age. These mice were severely growth restricted and exhibited spontaneous seizure activity and severe hypoglycemia. Thus, all subsequent experiments were performed on healthy mice that survived beyond 4 weeks of age. Experiments were performed with mice of adiposities similar to those of weight-matched nonlittermate controls.

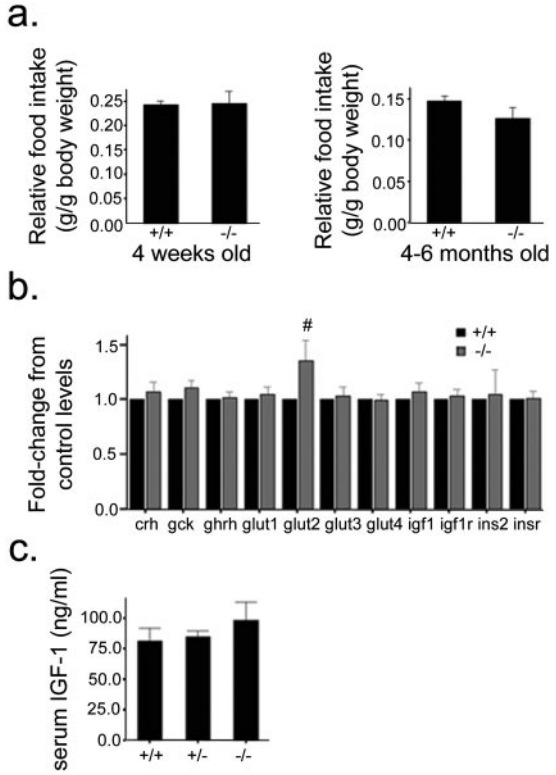

FIG. 3. Growth restriction in RIP*cre*$^{+}$ *Pten*$^{fl/fl}$ mice is not due to altered food intake or the GH/IGF-1 axis. (a) Food intake levels are similar between RIP*cre*$^{+}$ *Pten*$^{fl/fl}$ and RIP*cre*$^{+}$ *Pten*$^{+/+}$ mice soon after weaning (left panel) and at 4 to 6 months of age (right panel). Daily food intake is normalized for body weight and expressed as relative food intake ($n = 4$ per genotype). (b) RT-PCR for various transcripts levels in isolated hypothalamus ($n \geq 8$; age, 8 to 12 weeks). #, $P = 0.098$. (c) Serum IGF-1 levels are similar in RIP*cre*$^{+}$ *Pten*$^{fl/fl}$ and RIP*cre*$^{+}$ *Pten*$^{+/+}$ or RIP*cre*$^{+}$ *Pten*$^{+/fl}$ mice ($n \geq 3$; age, 5 to 8 weeks old). Error bars indicate standard errors of the means. +/+, RIP*cre*$^{+}$ *Pten*$^{+/+}$ mice; −/−, RIP*cre*$^{+}$ *Pten*$^{fl/fl}$ mice; +/−, RIP*cre*$^{+}$ *Pten*$^{+/fl}$ mice.

RIP*cre*$^{+}$ *Pten*$^{fl/fl}$ mice consumed amounts of chow (controlled for their lower weight) similar to those consumed by their RIP*cre*$^{+}$ *Pten*$^{+/+}$ littermates (Fig. 3a). Given the importance of the GH/IGF-1 axis in postnatal growth (43), we examined hypothalamic and systemic levels of these hormones.

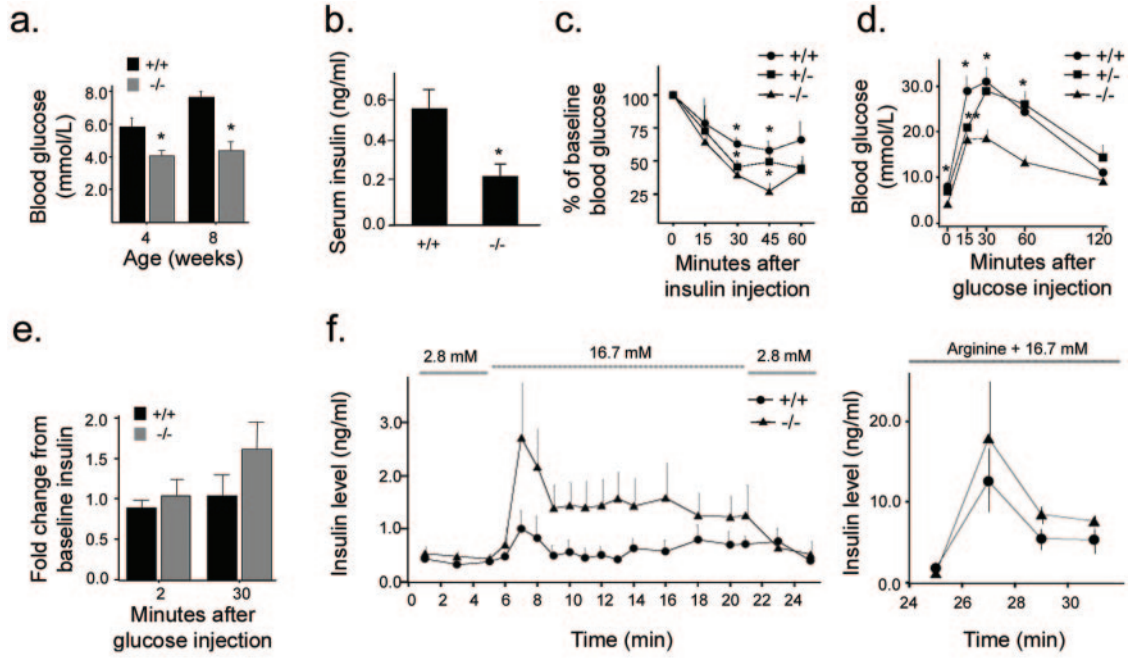

FIG. 4. Glucose metabolism and insulin secretion. (a) Fasting blood glucose levels in RIP*cre*$^+$ *Pten*$^{fl/fl}$ mice are lower than those in littermate RIP*cre*$^+$ *Pten*$^{+/+}$ controls ($n \geq 8$). *, $P \leq 0.005$. (b) Systemic-fasting serum insulin levels are lower in RIP*cre*$^+$ *Pten*$^{fl/fl}$ mice ($n \geq 6$). *, $P \leq 0.05$. (c) Insulin tolerance tests demonstrate greater insulin sensitivity in RIP*cre*$^+$ *Pten*$^{fl/fl}$ mice. The hypoglycemic response to an i.p. injection of human regular insulin at a dose of 0.5 mU/g of body weight is expressed as a percentage of baseline blood glucose ($n \geq 3$; age, 8 to 10 weeks). *, $P < 0.05$. (d) RIP*cre*$^+$ *Pten*$^{fl/fl}$ mice have lower glucose excursions after i.p. glucose tolerance tests compared with that for RIP*cre*$^+$ *Pten*$^{+/+}$ and RIP*cre*$^+$ *Pten*$^{+/fl}$ mice ($n \geq 4$; age, 2 to 4 months). *, $P < 0.005$ for comparison of RIP*cre*$^+$ *Pten*$^{fl/fl}$ versus RIP*cre*$^+$ *Pten*$^{+/+}$ or RIP*cre*$^+$ *Pten*$^{+/fl}$; **, $P = 0.011$ for RIP*cre*$^+$ *Pten*$^{+/fl}$ versus RIP*cre*$^+$ *Pten*$^{+/+}$ and $P = 0.042$ for RIP*cre*$^+$ *Pten*$^{+/fl}$ versus RIP*cre*$^+$ *Pten*$^{fl/fl}$. (e) In vivo glucose-stimulated insulin secretion after i.p. glucose injection at 2 and 30 min is preserved. *P* was not significant. (f) Insulin secretion in isolated perfused pancreas. The left panel shows the response to glucose at the molar concentrations indicated. The right panel shows the response to arginine and 16.7 mM glucose. *P* was not significant for all time points. Error bars indicate standard errors of the means. +/+, RIP*cre*$^+$ *Pten*$^{+/+}$ mice; −/−, RIP*cre*$^+$ *Pten*$^{fl/fl}$ mice; +/−, RIP*cre*$^+$ *Pten*$^{+/fl}$ mice.

Transcript levels of growth hormone-releasing hormone, IGF-1, or IGF-1 receptor did not differ between RIP*cre*$^+$ *Pten*$^{fl/fl}$ and RIP*cre*$^+$ *Pten*$^{+/+}$ mice (Fig. 3b). Similarly, circulating serum IGF-1 levels were not significantly different between RIP*cre*$^+$ *Pten*$^{fl/fl}$ and RIP*cre*$^+$ *Pten*$^{+/+}$ mice (Fig. 3c). This result is in keeping with the notion that circulating IGF-1 levels per se do not determine body growth (44). Similarly, serum GH and corticosterone levels measured following an overnight fast did not differ between RIP*cre*$^+$ *Pten*$^{fl/fl}$ mice and littermate controls (data not shown). Thus, PTEN deletion mediated by RIP*cre* resulted in a profound postnatal growth defect and shortened life span without having a significant impact on hypothalamic or systemic GH and IGF-1 hormone levels.

Improved insulin sensitivity and glucose tolerance in RIPcre$^+$ *Pten*$^{fl/fl}$ mice, with preserved β-cell function. In order to assess the impact of PTEN deletion on whole-body glucose metabolism, RIP*cre*$^+$ *Pten*$^{fl/fl}$ mice were fasted overnight and blood glucose and serum insulin levels were measured. RIP*cre*$^+$ *Pten*$^{fl/fl}$ mice had lower fasting blood glucose and insulin levels than did RIP*cre*$^+$ *Pten*$^{+/+}$ mice (Fig. 4a and b), suggestive of greater insulin sensitivity. Insulin tolerance tests did indeed show a more marked glucose-lowering response to i.p. insulin injection in these mice (Fig. 4c). In keeping with enhanced insulin sensitivity, RIP*cre*$^+$ *Pten*$^{fl/fl}$ mice exhibited lower glucose excursions after i.p. glucose injection (Fig. 4d). Furthermore, insulin secretion in response to an i.p. glucose challenge was intact in vivo (Fig. 4e). In order to examine β-cell function independently of the contributions of in vivo systemic insulin sensitivity, whole-pancreas perfusion studies were performed. Pancreata of RIP*cre*$^+$ *Pten*$^{fl/fl}$ mice continued to demonstrate intact insulin secretions in response to glucose; the response to arginine was also preserved (Fig. 4f). These data show that RIP*cre*$^+$ *Pten*$^{fl/fl}$ mice have increased whole-body insulin sensitivity and preserved β-cell functional capacity.

Deletion of PTEN in β cells leads to increased islet mass without tumorigenesis. To further explore the effects of PTEN on β-cell capacity, we next examined pancreatic islet morphology. RIP*cre*$^+$ *Pten*$^{fl/fl}$ mice showed an increase in total islet area (Fig. 5a). The increase in β-cell mass was due to both increased β-cell size (Fig. 5b) and β-cell numbers, with a 1.2- to 1.7-fold increase in islet number per pancreatic section in RIP*cre*$^+$ *Pten*$^{fl/fl}$ mice. This increase spanned across all sizes of islets to similar degrees, suggesting that there was both expansion of existing islets as well as islet neogenesis. Consistent with the enhanced β-cell mass, total pancreatic insulin content was increased in the RIP*cre*$^+$ *Pten*$^{fl/fl}$ mice (Fig. 5c). The increased β-cell mass observed in the RIP*cre*$^+$ *Pten*$^{fl/fl}$ mice is quite striking given their greater insulin sensitivity and low serum insulin levels. Furthermore, the increased β-cell mass in RIP*cre*$^+$ *Pten*$^{fl/fl}$ mice was not accompanied by evidence of

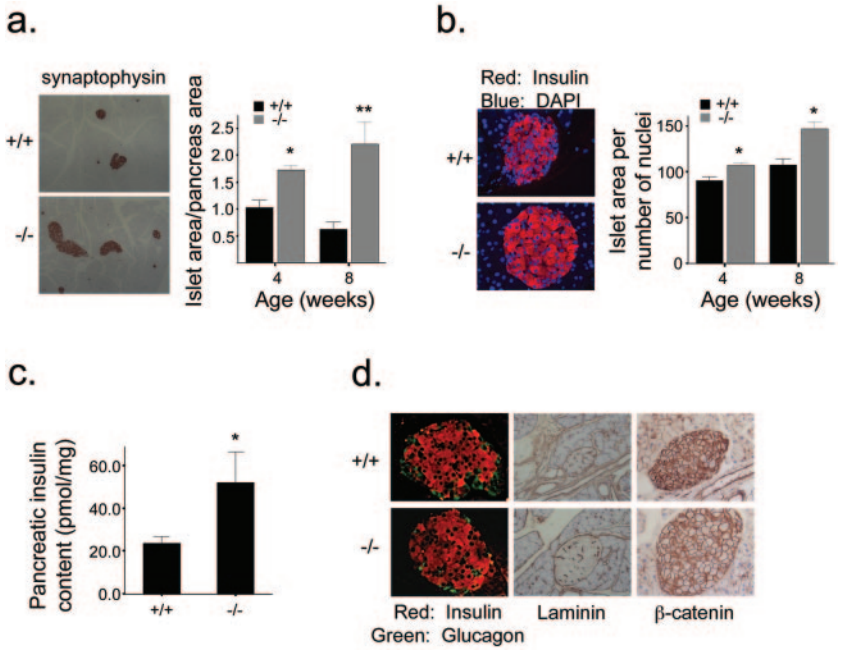

FIG. 5. Islet morphology and function. (a) Increased total islet area in RIP*cre*$^{+}$ *Pten*$^{fl/fl}$ mice compared with that in littermate RIP*cre*$^{+}$ *Pten*$^{+/+}$ mice shown by immunohistochemistry of representative pancreatic sections stained for synaptophysin (left panels; original magnification, ×4) and expressed as a percentage of total pancreatic area (right panel, synaptophysin stained area divided by total pancreatic area) ($n \geq 7$). *, $P = 0.015$; **, $P = 0.028$. (b) β-Cell size is increased in islets of RIP*cre*$^{+}$ *Pten*$^{fl/fl}$ mice compared with that in the islets of RIP*cre*$^{+}$ *Pten*$^{+/+}$ littermates, costained for insulin and DAPI (left panels; original magnification, ×40) and expressed as a ratio of insulin-stained area to number of nuclei within insulin-stained area (right panel) ($n \geq 7$). *, $P \leq 0.005$. (c) Total pancreatic insulin content is increased in RIPcre^{+} *Pten*$^{fl/fl}$ mice compared to that in RIP*cre*$^{+}$ *Pten*$^{+/+}$ mice, ($n \geq 3$; age, 8 to 12 weeks). *, $P = 0.029$. (d) Islet architecture is preserved without evidence of tumorigenesis. Insulin and glucagon staining show normal β- and α-cell distributions (original magnification, ×20), basement membranes are intact as shown by laminin staining (original magnification, ×10), and β-catenin localizes to the cell membrane (original magnification, ×20), demonstrating intact cell-to-cell adhesion. Error bars indicate standard errors of the means. +/+, RIP*cre*$^{+}$ *Pten*$^{+/+}$ mice; −/−, RIP*cre*$^{+}$ *Pten*$^{fl/fl}$ mice.

deregulated growth. When the mice were examined at 2 months of age (Fig. 5d) or at 8 to 9 months of age (data not shown), normal distribution and proportions of β and α cells were observed. There was no evidence of invasiveness of islet tissue. Intact laminin staining as well as the localization of β-catenin to the plasma membrane was present, consistent with preserved islet basement membrane structures and intact cell-cell adhesion, respectively. Thus, PTEN deletion in β cells has a direct effect on increasing β-cell mass without tumor formation while maintaining exquisite physiological β-cell function.

β Cells from RIPcre^{+} *Pten*$^{fl/fl}$ mice tend to have increased proliferation and are protected from streptozotocin-induced diabetes development. In order to elucidate the cellular processes that resulted in increased β-cell mass, we first assessed proliferation by examining Ki67 expression in islets of pancreatic sections. There was a trend toward increased proliferation of β cells in RIP*cre*$^{+}$ *Pten*$^{fl/fl}$ mice (Fig. 6a). That the difference was not statistically significant is likely due to the inherently low rates of β-cell proliferation that occur under static conditions (4). Similarly, rates of apoptosis under static conditions, as examined by TUNEL staining, were also low and not significantly different between RIP*cre*$^{+}$ *Pten*$^{fl/fl}$ mice and RIP*cre*$^{+}$ *Pten*$^{+/+}$ controls (data not shown). In order to examine whether PTEN deletion in β cells would provide protection against β-cell apoptosis in stimulated conditions, we used the experimental diabetes model induced by MLDS (22). The RIP*cre*$^{+}$ *Pten*$^{fl/fl}$ mice were protected from the development of diabetes after MLDS injections (Fig. 6b). An examination of the pancreata following diabetes induction in the control mice revealed fewer TUNEL-positive nuclei in the RIP*cre*$^{+}$ *Pten*$^{fl/fl}$ mice (Fig. 6c), suggesting that the RIP*cre*$^{+}$ *Pten*$^{fl/fl}$ mice were protected from β-cell apoptosis. Thus, PTEN deletion in β cells confers protection against MLDS-induced diabetes.

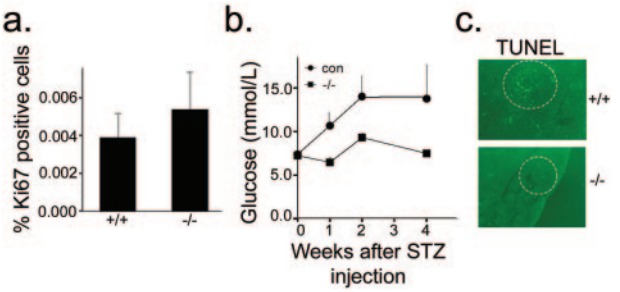

FIG. 6. β-Cell proliferation and apoptosis. (a) RIP*cre*$^{+}$ *Pten*$^{fl/fl}$ mice tend to have a higher percentage of Ki67-positive cells than do their RIP*cre*$^{+}$ *Pten*$^{+/+}$ littermates ($n = 8$ per genotype). (b) Effect of MLDS on blood glucose levels showing protection against MLDS-induced diabetes in RIP*cre*$^{+}$ *Pten*$^{fl/fl}$ mice ($n = 2$ to 5; age, 7 to 9 weeks). con, control; STZ, streptozotocin. (c) Representative islets of MLDS-treated RIP*cre*$^{+}$ *Pten*$^{fl/fl}$ and RIP*cre*$^{+}$ *Pten*$^{+/+}$ mice stained for TUNEL, showing fewer TUNEL-positive nuclei in RIP*cre*$^{+}$ *Pten*$^{fl/fl}$ mice. +/+, RIP*cre*$^{+}$ *Pten*$^{+/+}$ mice; −/−, RIP*cre*$^{+}$ *Pten*$^{fl/fl}$ mice.

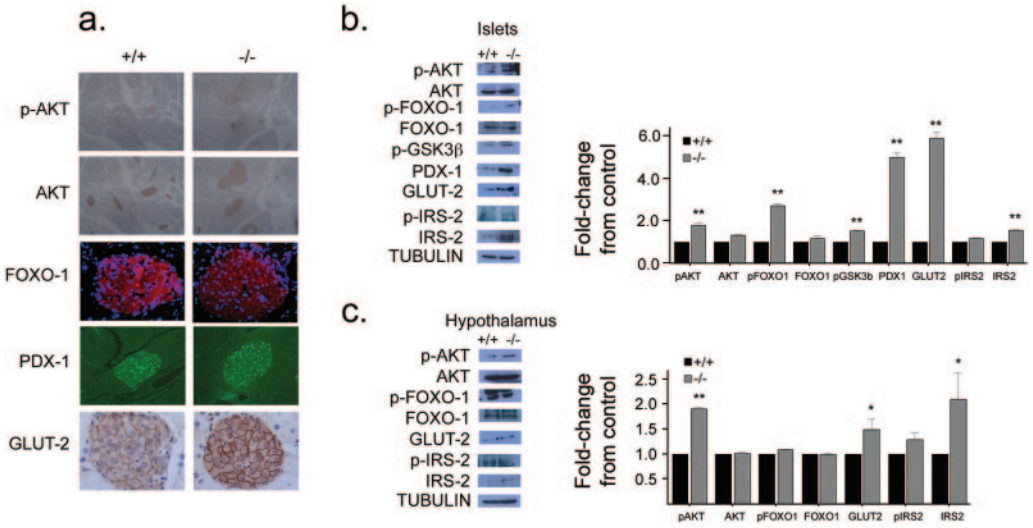

FIG. 7. Effect of *Pten* deletion on the insulin/IGF-1 signaling pathway. (a) Immunohistochemistry of pancreatic sections shows that RIP*cre*$^{+}$ *Pten*$^{fl/fl}$ mice have increased phospho-AKT, cytoplasmic localization of FoxO-1, increased nuclear PDX-1, and increased GLUT2. (b) Western blots (left panel) and quantification (right panel) of isolated islets showing that absence of PTEN in β cells leads to increased phospho-AKT, FoxO-1, and GSK3β as well as enhanced PDX-1, GLUT2, and IRS-2 levels. **, $P < 0.005$. (c) Western blots (left panel) and quantification (right panel) from isolated hypothalamus showing that partial deletion of PTEN leads to enhanced phospho-AKT, similar levels of phospho- and total FoxO-1, and elevated GLUT2 and IRS-2 expression in RIP*cre*$^{+}$ *Pten*$^{fl/fl}$ mice. *, $P < 0.05$; **, $P < 0.005$. Error bars indicate standard errors of the means. p, phospho; +/+, RIP*cre*$^{+}$ *Pten*$^{+/+}$ mice; −/−, RIP*cre*$^{+}$ *Pten*$^{fl/fl}$ mice.

Disruption of PTEN leads to enhanced insulin/IGF-1 signaling in β cells and hypothalamus. To determine the mechanisms for the changes in growth, metabolism, and β-cell homeostasis in vivo, we assessed the effect of tissue-specific PTEN deletion on the insulin/IGF-1 signaling cascade in isolated islets and hypothalamus following an overnight fast. PTEN deletion resulted in increased AKT phosphorylation in β cells (Fig. 7a and b) as well as hypothalamus (Fig. 7c), suggesting constitutive activation of the PI3K pathway. FoxO-1 and GSK3β, evolutionarily conserved substrates of AKT, also showed increased phosphorylation in these islets (Fig. 7b). The phosphorylation of FoxO-1 prevents its nuclear entry (1); thus, immunofluorescence showed cytoplasmic localization of FoxO-1 (Fig. 7a). In keeping with the observation of enhanced insulin signaling, the islets of RIP*cre*$^{+}$ *Pten*$^{fl/fl}$ mice showed greater expression and nuclear localization of PDX-1, a downstream transcriptional target of insulin signaling that is important for β-cell growth and differentiation (18) (Fig. 7a and b). Furthermore, GLUT2, a β-cell differentiation marker, was also increased at the cell membrane in RIP*cre*$^{+}$ *Pten*$^{fl/fl}$ mice (Fig. 7a and b). Interestingly, GLUT2 was also increased in the hypothalamus (Fig. 7c). IRS-2, which signals proximal to PTEN, was also increased in total protein levels in hypothalamus and islets of RIP*cre*$^{+}$ *Pten*$^{fl/fl}$ mice, suggesting that PTEN deletion leads to a positive amplification of signaling. Thus, PTEN deletion driven by the insulin promoter results in the augmentation of the insulin/IGF-1-PI3K signaling pathway in β cells and hypothalamus.

DISCUSSION

Given the unique virtues of β cells in both proliferative and functional capacities as well as the diverse functions of PTEN, it was not clear what roles PTEN may have had in β cells. Since PTEN functions in a highly context-dependent manner, its function in β cells would be difficult to address in a globally targeted model (20). We observed significant increases in islet area and β-cell size as a result of PTEN deletion within β cells. Notably, the magnitude of increase in β-cell mass was not to the extent of transgenic constitutive overexpression of protein kinase B/AKT (3, 40), thereby highlighting the critical nature of physiologic inhibitory signals conferred by PTEN.

Importantly, increased β-cell mass in the RIP*cre*$^{+}$ *Pten*$^{fl/fl}$ mice did not progress to tumor formation. In fact, the differentiated β-cell function was not at all compromised in these mice. Our data are the first to look systematically at β-cell function in the absence of PTEN, and we have shown an intact response to glucose in vivo and a preserved robust response to both glucose and arginine when stimulated in isolated pancreas. Additionally, despite the increase in β-cell mass and pancreatic insulin content, plasma insulin levels remained low as a consequence of lesser insulin requirements, further highlighting the preservation of intact glucose-sensing capacity in this expanded β-cell population.

Of note, while this work was under review, another group published similar β-cell findings with targeted deletion of PTEN utilizing the RIP*cre*$^{+}$ system (37). In particular, they also found the deletion of PTEN in β cells to lead to increased islet mass without tumorigenesis. Additionally, they found lower fasting glucose levels in mutant mice, with intact insulin secretory capacities in vitro. Similar to our findings, PTEN deletion in β cells conferred protection against streptozotocin-induced diabetes. Since both type 1 and type 2 diabetes are diseases where deficiencies in β-cell mass and function are pathogenic, the role of PTEN in β cells to increase islet mass without loss of differentiated function makes PTEN an attractive molecular target for future therapies for diabetes.

The deletion of PTEN directed by the insulin promoter resulted in the efficient deletion of PTEN in pancreatic β cells and the partial deletion of PTEN in the hypothalamus. The degree of disruption of PTEN expression in these tissues was in keeping with the magnitude of deletion in other reports using tissue-targeted ablation directed by RIP (15, 23). The diminished expression of PTEN in the hypothalamus uncovers a potentially novel role for PTEN in the insulin-transcribing neuronal cells. However, this population of hypothalamic neurons remains as yet not fully characterized but does appear to be distinct from other more well-defined hypothalamic neurons, such as the pro-opiomelanocortin and neuropeptide Y neurons (6).

We attribute the growth restriction in our RIP*cre*$^{+}$ *Pten*$^{fl/fl}$ mice to hypothalamic PTEN deletion. Our findings are supported by Stiles et al.; they also found postnatal growth restriction of a magnitude similar to that of our RIP*cre*$^{+}$ *Pten*$^{fl/fl}$ mice (37). The attribution of the body size phenotype to hypothalamic PTEN rather than PTEN function in β cells is in keeping with a recent report where PTEN deleted specifically in the pancreas using the PDX promoter did not show any defect in body size (34). In this model, when PTEN was developmentally deleted by PDX*cre*, the mice developed pancreatic acinar tumors, whereas deletion in adult islets using the inducible PDX*cre* system led to islet hyperplasia but no body size phenotype. Additionally, it is likely that the growth restriction depends on the developmental deletion of PTEN in the hypothalamus, since PTEN deletion in adult hypothalamus using *Cre* adenovirus injection did not lead to growth restriction (37).

Insulin/IGF-1 signaling is associated with growth, ageing, stress response, and reproduction across all species (28). The dampening of this signaling pathway in *Caenorhabditis elegans* or *Drosophila melanogaster* genetically or by nutrient restriction leads to small body size and longevity (24, 39). Thus, the small-body phenotype in the RIP*cre*$^{+}$ *Pten*$^{fl/fl}$ mice is surprising, given the observed enhanced PI3K signaling in both the hypothalamus and β cells. This finding highlights the extreme context dependency of PTEN function, as neuronal PTEN deletion driven by glial fibrillary acidic protein (2) or nestin promoters (11) do not affect body size.

We observed neither a decrease of circulating GH or IGF-1 levels nor a change in hypothalamic growth hormone-releasing hormone transcript levels in the RIP*cre*$^{+}$ *Pten*$^{fl/fl}$ mice. These data suggest that the growth restriction in the RIP*cre*$^{+}$ *Pten*$^{fl/fl}$ mice is not due to perturbations in the GH/IGF-1 axis. However, our data do not assess the bioactivity of these hormones. Thus, the complex roles of these hormones that function in an integrated autocrine, paracrine, and endocrine manner may still be ultimately affected in our mouse model.

The enhanced insulin sensitivity observed in the RIP*cre*$^{+}$ *Pten*$^{fl/fl}$ mice is most likely due to the partial loss of PTEN in the hypothalamus. Our findings are in contrast to that of Stiles et al. (37). That group found no difference in insulin sensitivity or fasting insulin levels in their mutant mice, which may be a reflection of the different genetic background of their mice. Our observation of enhanced insulin sensitivity is in keeping with the emerging notion that the hypothalamus is important for both sensing and responding to nutrients and hormonal signals that gauge metabolic status (27, 31). Additionally, the hypothalamus directs metabolic homeostasis by neuronal and hormonal output signals that are still unknown. The PI3K pathway is emerging as a key player in these processes (25, 26). Our data suggest that PTEN may be another key player in the PI3K pathway that determines metabolic homeostasis.

One approach to test the role of PTEN function in hypothalamic neurons of RIP*cre*$^{+}$ *Pten*$^{fl/fl}$ mice would be to utilize centrally administered PI3K inhibitors to try to restore growth or insulin resistance to control levels. However, this method would be difficult given the small body size and relative fragility of the RIP*cre*$^{+}$ *Pten*$^{fl/fl}$ mice. Additionally, such an approach would not specifically inhibit PI3K in the neurons of interest; adjacent neurons would also be affected. Therefore, full elucidation of the roles of these insulin-transcribing neurons in growth and metabolism must await better characterization of their structure and development of genetic techniques to specifically manipulate them.

In summary, we have shown that the deletion of PTEN in tissues transcribing insulin resulted in enhanced insulin/IGF-1 signaling, with manifestations in whole-body growth, improved insulin sensitivity, increased β-cell mass, and preserved β-cell function. Our findings highlight the importance of the negative regulation that is provided by PTEN in vivo. These findings emphasize the essential physiological roles of PTEN and give important guidance for potential development of tissue- or cell-type-specific therapies in integrated strategies to target insulin resistance and β-cell defects.

ACKNOWLEDGMENTS

This work was supported by grants to M.W. from the Canadian Institutes of Health Research and the Canadian Diabetes Association. M.W. is a CIHR and Banting and Best Diabetes Centre New Investigator. K.-T.T.N. is supported by a postdoctoral fellowship from the Keenan Foundation.

We thank Loretta Lam, Adria Giacca, Rene Mader, Shereen Ezzat, and Lesley Wu for technical assistance and Paul Doherty for critical editing of the manuscript.

REFERENCES

1. **Accili, D., and K. C. Arden.** 2004. FoxOs at the crossroads of cellular metabolism, differentiation, and transformation. Cell **117:**421–426.
2. **Backman, S. A., V. Stambolic, A. Suzuki, J. Haight, A. Elia, J. Pretorius, M. S. Tsao, P. Shannon, B. Bolon, G. O. Ivy, and T. W. Mak.** 2001. Deletion of *Pten* in mouse brain causes seizures, ataxia and defects in soma size resembling Lhermitte-Duclos disease. Nat. Genet. **29:**396–403.
3. **Bernal-Mizrachi, E., W. Wen, S. Stahlhut, C. M. Welling, and M. A. Permutt.** 2001. Islet beta cell expression of constitutively active Akt1/PKB alpha induces striking hypertrophy, hyperplasia, and hyperinsulinemia. J. Clin. Invest. **108:** 1631–1638.
4. **Bonner-Weir, S., and G. C. Weir.** 2005. New sources of pancreatic beta-cells. Nat. Biotechnol. **23:**857–861.
5. **Butler, M., R. A. McKay, I. J. Popoff, W. A. Gaarde, D. Witchell, S. F. Murray, N. M. Dean, S. Bhanot, and B. P. Monia.** 2002. Specific inhibition of PTEN expression reverses hyperglycemia in diabetic mice. Diabetes **51:** 1028–1034.
6. **Choudhury, A. I., H. Heffron, M. A. Smith, H. Al-Qassab, A. W. Xu, C. Selman, M. Simmgen, M. Clements, M. Claret, G. Maccoll, D. C. Bedford, K. Hisadome, I. Diakonov, V. Moosajee, J. D. Bell, J. R. Speakman, R. L. Batterham, G. S. Barsh, M. L. Ashford, and D. J. Withers.** 2005. The role of insulin receptor substrate 2 in hypothalamic and beta cell function. J. Clin. Investig. **115:**940–950.
7. **Crackower, M. A., G. Y. Oudit, I. Kozieradzki, R. Sarao, H. Sun, T. Sasaki, E. Hirsch, A. Suzuki, T. Shioi, J. Irie-Sasaki, R. Sah, H. Y. Cheng, V. O. Rybin, G. Lembo, L. Fratta, A. J. Oliveira-dos-Santos, J. L. Benovic, C. R. Kahn, S. Izumo, S. F. Steinberg, M. P. Wymann, P. H. Backx, and J. M. Penninger.** 2002. Regulation of myocardial contractility and cell size by distinct PI3K-PTEN signaling pathways. Cell **110:**737–749.
8. **Darwiche, R., M. M. Chong, P. Santamaria, H. E. Thomas, and T. W. Kay.** 2003. Fas is detectable on beta cells in accelerated, but not spontaneous, diabetes in nonobese diabetic mice. J. Immunol. **170:**6292–6297.
9. **Gannon, M., C. Shiota, C. Postic, C. V. Wright, and M. Magnuson.** 2000.

Analysis of the Cre-mediated recombination driven by rat insulin promoter in embryonic and adult mouse pancreas. Genesis **26:**139–142.
10. **Gerozissis, K.** 2003. Brain insulin: regulation, mechanisms of action and functions. Cell. Mol. Neurobiol. **23:**1–25.
11. **Groszer, M., R. Erickson, D. D. Scripture-Adams, R. Lesche, A. Trumpp, J. A. Zack, H. I. Kornblum, X. Liu, and H. Wu.** 2001. Negative regulation of neural stem/progenitor cell proliferation by the *Pten* tumor suppressor gene in vivo. Science **294:**2186–2189.
12. **Hennige, A. M., D. J. Burks, U. Ozcan, R. N. Kulkarni, J. Ye, S. Park, M. Schubert, T. L. Fisher, M. A. Dow, R. Leshan, M. Zakaria, M. Mossa-Basha, and M. F. White.** 2003. Upregulation of insulin receptor substrate-2 in pancreatic beta cells prevents diabetes. J. Clin. Investig. **112:**1521–1532.
13. **Horie, Y., A. Suzuki, E. Kataoka, T. Sasaki, K. Hamada, J. Sasaki, K. Mizuno, G. Hasegawa, H. Kishimoto, M. Iizuka, M. Naito, K. Enomoto, S. Watanabe, T. W. Mak, and T. Nakano.** 2004. Hepatocyte-specific Pten deficiency results in steatohepatitis and hepatocellular carcinomas. J. Clin. Investig. **113:**1774–1783.
14. **Joseph, J. W., V. Koshkin, C. Y. Zhang, J. Wang, B. B. Lowell, C. B. Chan, and M. B. Wheeler.** 2002. Uncoupling protein 2 knockout mice have enhanced insulin secretory capacity after a high-fat diet. Diabetes **51:**3211–3219.
15. **Kubota, N., Y. Terauchi, K. Tobe, W. Yano, R. Suzuki, K. Ueki, I. Takamoto, H. Satoh, T. Maki, T. Kubota, M. Moroi, M. Okada-Iwabu, O. Ezaki, R. Nagai, Y. Ueta, T. Kadowaki, and T. Noda.** 2004. Insulin receptor substrate 2 plays a crucial role in beta cells and the hypothalamus. J. Clin. Investig. **114:**917–927.
16. **Kulkarni, R. N., J. C. Bruning, J. N. Winnay, C. Postic, M. A. Magnuson, and C. R. Kahn.** 1999. Tissue-specific knockout of the insulin receptor in pancreatic beta cells creates an insulin secretory defect similar to that in type 2 diabetes. Cell **96:**329–339.
17. **Kulkarni, R. N., M. Holzenberger, D. Q. Shih, U. Ozcan, M. Stoffel, M. A. Magnuson, and C. R. Kahn.** 2002. Beta-cell-specific deletion of the Igf1 receptor leads to hyperinsulinemia and glucose intolerance but does not alter beta-cell mass. Nat. Genet. **31:**111–115.
18. **Kulkarni, R. N., U. S. Jhala, J. N. Winnay, S. Krajewski, M. Montminy, and C. R. Kahn.** 2004. PDX-1 haploinsufficiency limits the compensatory islet hyperplasia that occurs in response to insulin resistance. J. Clin. Investig. **114:**828–836.
19. **Kurlawalla-Martinez, C., B. Stiles, Y. Wang, S. U. Devaskar, B. B. Kahn, and H. Wu.** 2005. Insulin hypersensitivity and resistance to streptozotocin-induced diabetes in mice lacking PTEN in adipose tissue. Mol. Cell. Biol. **25:**2498–2510.
20. **Kushner, J. A., L. Simpson, L. M. Wartschow, S. Guo, M. M. Rankin, R. Parsons, and M. F. White.** 2005. *Pten* regulation of islet growth and glucose homeostasis. J. Biol. Chem. **280:**39388–39393.
21. **Liadis, N., K. Murakami, M. Eweida, A. R. Elford, L. Sheu, H. Y. Gaisano, R. Hakem, P. S. Ohashi, and M. Woo.** 2005. Caspase-3-dependent beta-cell apoptosis in the initiation of autoimmune diabetes mellitus. Mol. Cell. Biol. **25:**3620–3629.
22. **Like, A. A., and A. A. Rossini.** 1976. Streptozotocin-induced pancreatic insulitis: new model of diabetes mellitus. Science **193:**415–417.
23. **Lin, X., A. Taguchi, S. Park, J. A. Kushner, F. Li, Y. Li, and M. F. White.** 2004. Dysregulation of insulin receptor substrate 2 in beta cells and brain causes obesity and diabetes. J. Clin. Investig. **114:**908–916.
24. **Longo, V. D., and C. E. Finch.** 2003. Evolutionary medicine: from dwarf model systems to healthy centenarians? Science **299:**1342–1346.
25. **Morton, G. J., R. W. Gelling, K. D. Niswender, C. D. Morrison, C. J. Rhodes, and M. W. Schwartz.** 2005. Leptin regulates insulin sensitivity via phosphatidylinositol-3-OH kinase signaling in mediobasal hypothalamic neurons. Cell Metab. **2:**411–420.
26. **Niswender, K. D., C. D. Morrison, D. J. Clegg, R. Olson, D. G. Baskin, M. G. Myers, Jr., R. J. Seeley, and M. W. Schwartz.** 2003. Insulin activation of phosphatidylinositol 3-kinase in the hypothalamic arcuate nucleus: a key mediator of insulin-induced anorexia. Diabetes **52:**227–231.
27. **Pocai, A., S. Obici, G. J. Schwartz, and L. Rossetti.** 2005. A brain-liver circuit regulates glucose homeostasis. Cell Metab. **1:**53–61.
28. **Porte, D., Jr., D. G. Baskin, and M. W. Schwartz.** 2005. Insulin signaling in the central nervous system: a critical role in metabolic homeostasis and disease from C. elegans to humans. Diabetes **54:**1264–1276.
29. **Postic, C., M. Shiota, K. D. Niswender, T. L. Jetton, Y. Chen, J. M. Moates, K. D. Shelton, J. Lindner, A. D. Cherrington, and M. A. Magnuson.** 1999. Dual roles for glucokinase in glucose homeostasis as determined by liver and pancreatic beta cell-specific gene knock-outs using Cre recombinase. J. Biol. Chem. **274:**305–315.
30. **Saltiel, A. R., and C. R. Kahn.** 2001. Insulin signalling and the regulation of glucose and lipid metabolism. Nature **414:**799–806.
31. **Schwartz, M. W., and D. Porte, Jr.** 2005. Diabetes, obesity, and the brain. Science **307:**375–379.
32. **Stambolic, V., A. Suzuki, J. L. de la Pompa, G. M. Brothers, C. Mirtsos, T. Sasaki, J. Ruland, J. M. Penninger, D. P. Siderovski, and T. W. Mak.** 1998. Negative regulation of PKB/Akt-dependent cell survival by the tumor suppressor PTEN. Cell **95:**29–39.
33. **Stambolic, V., M. S. Tsao, D. Macpherson, A. Suzuki, W. B. Chapman, and T. W. Mak.** 2000. High incidence of breast and endometrial neoplasia resembling human Cowden syndrome in pten$^{+/-}$ mice. Cancer Res. **60:**3605–3611.
34. **Stanger, B. Z., B. Stiles, G. Y. Lauwers, N. Bardeesy, M. Mendoza, Y. Wang, A. Greenwood, K. H. Cheng, M. McLaughlin, D. Brown, R. A. Depinho, H. Wu, D. A. Melton, and Y. Dor.** 2005. *Pten* constrains centroacinar cell expansion and malignant transformation in the pancreas. Cancer Cell **8:**185–195.
35. **Steck, P. A., M. A. Pershouse, S. A. Jasser, W. K. Yung, H. Lin, A. H. Ligon, L. A. Langford, M. L. Baumgard, T. Hattier, T. Davis, C. Frye, R. Hu, B. Swedlund, D. H. Teng, and S. V. Tavtigian.** 1997. Identification of a candidate tumour suppressor gene, MMAC1, at chromosome 10q23.3 that is mutated in multiple advanced cancers. Nat. Genet. **15:**356–362.
36. **Stiles, B., Y. Wang, A. Stahl, S. Bassilian, W. P. Lee, Y. J. Kim, R. Sherwin, S. Devaskar, R. Lesche, M. A. Magnuson, and H. Wu.** 2004. Liver-specific deletion of negative regulator Pten results in fatty liver and insulin hypersensitivity Proc. Natl. Acad. Sci. USA **101:**2082–2087.
37. **Stiles, B. L., C. Kuralwalla-Martinez, W. Guo, C. Gregorian, Y. Wang, J. Tian, M. A. Magnuson, and H. Wu.** 2006. Selective deletion of *Pten* in pancreatic β cells leads to increased islet mass and resistance to STZ-induced diabetes. Mol. Cell. Biol. **26:**2772–2781.
38. **Suzuki, A., T. Kaisho, M. Ohishi, M. Tsukio-Yamaguchi, T. Tsubata, P. A. Koni, T. Sasaki, T. W. Mak, and T. Nakano.** 2003. Critical roles of Pten in B cell homeostasis and immunoglobulin class switch recombination. J. Exp. Med. **197:**657–667.
39. **Tatar, M., A. Bartke, and A. Antebi.** 2003. The endocrine regulation of aging by insulin-like signals. Science **299:**1346–1351.
40. **Tuttle, R. L., N. S. Gill, W. Pugh, J. P. Lee, B. Koeberlein, E. E. Furth, K. S. Polonsky, A. Naji, and M. J. Birnbaum.** 2001. Regulation of pancreatic beta-cell growth and survival by the serine/threonine protein kinase Akt1/PKBα. Nat. Med. **7:**1133–1137.
41. **Wijesekara, N., D. Konrad, M. Eweida, C. Jefferies, N. Liadis, A. Giacca, M. Crackower, A. Suzuki, T. W. Mak, C. R. Kahn, A. Klip, and M. Woo.** 2005. Muscle-specific Pten deletion protects against insulin resistance and diabetes. Mol. Cell. Biol. **25:**1135–1145.
42. **Withers, D. J., J. S. Gutierrez, H. Towery, D. J. Burks, J. M. Ren, S. Previs, Y. Zhang, D. Bernal, S. Pons, G. I. Shulman, S. Bonner-Weir, and M. F. White.** 1998. Disruption of IRS-2 causes type 2 diabetes in mice. Nature **391:**900–904.
43. **Yakar, S., H. Kim, H. Zhao, Y. Toyoshima, P. Pennisi, O. Gavrilova, and D. Leroith.** 2005. The growth hormone-insulin like growth factor axis revisited: lessons from IGF-1 and IGF-1 receptor gene targeting. Pediatr. Nephrol. **20:**251–254.
44. **Yakar, S., J. L. Liu, B. Stannard, A. Butler, D. Accili, B. Sauer, and D. LeRoith.** 1999. Normal growth and development in the absence of hepatic insulin-like growth factor I. Proc. Natl. Acad. Sci. USA **96:**7324–7329.